phys. stat. sol. (b) **241**, No. 11, 2629–2638 (2004) / **DOI** 10.1002/pssb.200402061

Structural study of ferroelectric and paraelectric phases in $PbK_2LiNb_5O_{15}$

Y. Gagou[1], **Ch. Muller**[2], **M.-A. Frémy**[2], **D. Mezzane**[3], **E. Elkaïm**[4], and **P. Saint-Grégoire**[*, 5]

[1] LPMC, Université de Picardie, 33, rue Saint-Leu, 80039 Amiens Cédex, France
[2] L2MP, UMR-CNRS 6137, Université de Toulon-Var, BP 132, 83957 La Garde Cédex, France
[3] F.S.T.G.-F.S.S. University Cadi Ayyad Marrakech, Morocco
[4] LURE – UMR CNRS 130 – Centre Universitaire Paris-Sud, BP 34, 91898 Orsay Cédex, France
[5] University of Bangui, Centr. Afr. Rep.; perm. address: 14, Av. F. Mistral, 34110 Frontignan, France

Received 6 February 2004, revised 20 April 2004, accepted 28 June 2004

PACS 61.10.Nz, 61.50.Ks, 77.80.Bh, 77.84.Dy

The structures of $PbK_2LiNb_5O_{15}$ showing the ferroelectricity below about 640 K have been studied in the paraelectric and ferroelectric phases by means of synchrotron X-ray powder diffraction. The data are analyzed with a Rietveld refinement method. It is found that the paraelectric structure and the ferroelectric one are of tetragonal and orthorhombic symmetry with *P*4/*mbm* and *Pba*2, respectively. The *Pba*2 structure gives a polar displacement along *c*-axis, whose direction is consistent with that deduced from dielectric measurements. The refined chemical occupancies of the cations Pb, K and Nb give the site-situation of these ions in the tunnels with square sections and pentagonal sections in each phase.

1 Introduction

The compound $PbK_2LiNb_5O_{15}$ belongs to the PKLN family, which crystallizes in the Tetragonal Tungsten Bronze (TTB) structure. This structure can be described as a framework of NbO_6 octahedra sharing corners, which reveals three kinds of tunnels of pentagonal (p), square (s) and triangular (t) sections [1–3]. The first two sites have a coordination number respectively of 15 and 12 and can be occupied by ions of large size. The third site which has a coordination number of 9 can be occupied only by small size ions [4].

The high temperature paraelectric phase of the TTB compounds is generally tetragonal [5] usually with the space group *P*4/*mbm*. The point group 4/*mmm* is lowered in several compounds of this family in such a way that a ferroelectric phase is stabilised at lower temperature, the polarisation being in most cases in the [001] direction and the corresponding phase is tetragonal or orthorhombic.

Among all the Pb-based ferroelectric compounds of TTB structure constructed from NbO_6 octahedra, the compound $PbNb_2O_6$ [6, 7] with ferroelectric transition temperature T_C = 833 K is the simplest and considered as the reference. It presents an orthorhombic distortion in the ferroelectric phase which would be due to the strong polarisability of the Pb^{2+} ion that involves a structural anisotropy (distortion of oxygen octahedra). The polar axis of $PbNb_2O_6$ compound is located in the perpendicular plane (**a**, **b**) to the direction of the tunnels that is related to the high concentration of Pb.

Another basic compound, $Pb_2KNb_5O_{15}$ [8] which may be described from the precedent by substitution of one Pb atom by two K atoms has a lower critical temperature T_C = 730 K. The polar axis in $Pb_2KNb_5O_{15}$ is also directed in (**a**, **b**) plane.

---

[*] Corresponding author: e-mail: stgreg@ferroix.net

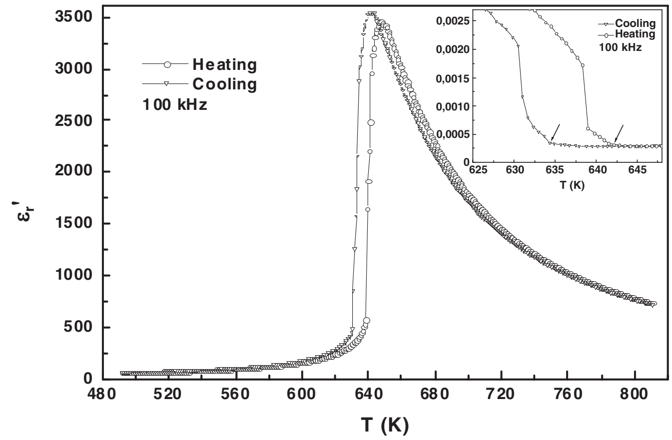

Fig. 1 Temperature dependence of the dielectric constant at 100 kHz (heating and cooling runs). The inset represents the $\varepsilon_r'^{-1}(T)$ variation nearby the phase transition showing the existence of a second anomaly indicated by arrows.

The new feature of the compound studied in the present paper ($PbK_2LiNb_5O_{15}$) is the **c**-orientation of the polar axis in ferroelectric phase. This compound can be described chemically by substitution of one of the Pb^{2+} cation by the couple of monovalent ions (K^+, Li^+) in $Pb_2KNb_5O_{15}$ compound. It appears from experiments on samples with a continuously varying composition, that the title compound has specific properties, and in particular a clear evidence of enhanced dielectric anomaly around 639 K exhibiting ferroelectricity (Fig. 1). However the phase change is more complicated than a single paraelectric-to-ferroelectric phase transition and, if a Curie law is followed far from the structural instability, there are clear deviations from it around 640 K, and an unusual behaviour associated with intermediate states or phases is observed [9–11]. Dielectric experiments show that the dielectric constant in the **c**-direction follows a Curie-Weiss law, consistent only with a polarization lying in **c**-direction.

This situation underlines the interest of determining the crystallographic structure in both phases, para- and ferro-electric to have information on the symmetry-breaking, the mechanism of the phase change, and the nature of change of atomic positions associated with ferroelectricity.

In this work, we present the results of refinements of synchrotron radiation diffraction diagram performed at 290 K and at 690 K using the Rietveld method [12], which allows us to solve the structural problem in both phases. The correspondence between high and low temperature structures is established.

2 Experimental

$PbK_2LiNb_5O_{15}$ powder is synthesised from oxides (PbO, Nb_2O_5) and carbonates (Li_2CO_3, K_2CO_3) of 99.99 % purity by solid state reaction according to the equation:

$$2\,PbO + 2\,K_2CO_3 + Li_2CO_3 + 5\,Nb_2O_5 \rightarrow 2\,PbK_2LiNb_5O_{15} + 3\,CO_2\,.$$

The starting materials were mixed in stoichiometric proportions and ground by ball milling in an aqueous solution for 24 hours. After the evaporation of water, the resulting powders were pressed under 4 bars to form cylinder-shaped pellets. These pellets were then fired successively at 1200, 1270 and 1320 K with grinding and X-ray diffraction control between each annealing. After numerous syntheses and trials, this way has appeared to give the best results, both for the chemical composition of the final product and its crystalline quality.

The structure of the paraelectric and ferroelectric phases of $PbK_2LiNb_5O_{15}$ has been refined from the fitting of high resolution data X-ray powder diffraction diagrams. The patterns were collected at room temperature (ferroelectric phase) and at 670 K (paraelectric phase) at LURE (Orsay – France) on the DW22 instrument. This line is equipped with a focussing monochromator constituted of two Si(111) crystals, which allows to select a beam with a very good monochromaticity (the used wavelength is 0.6918(1) Å). The high-resolution Debye-Scherrer geometry, using a rotating sample in a capillary tube, reduces the effect of preferential orientation and increases the number of grains in diffraction condition.

The analyzer allows a good angular resolution (about 0.02° in 2θ at small angles) and an improved signal/noise ratio. It is thus possible to get accurate information from the diffraction profile, in particular because intensities are obtained with a very good accuracy.

From the Rietveld refinements, the overall composition is confirmed and the distribution of the Pb^{2+} and K^+ cations over the square and pentagonal sites is determined. During refinements, all classical hypotheses concerning atomic positions (including the possibility of disorder) have been analyzed. In the following, we present briefly the results, by focusing mainly on those corresponding to the solution of the structural problem.

3 Results of high resolution X-ray powder diffraction

3.1 Paraelectric phase

3.1.1 Diffraction pattern

Before starting the structural refinement of the paraelectric phase, a careful analysis of the diffraction pattern registered at 670 K was done. This revealed a slight broadening of the (00ℓ) Bragg reflections.

We have performed peak fitting on a small angular domain (19.6–0.4° in 2θ) either by constraining all the full widths at half maximum to be equal or introducing a slight broadening for the (002) Bragg reflection. The best fit is obtained when there is no constraint on the widths and we get then for the (002) reflection a 2θ-value of 0.0284° instead of 0.0247° for the (620) and (540) reflections. Such a phenomenon was also observed for the (001) and (003) reflections.

To determine the exact origin of this broadening of the (00ℓ) lines, we analysed all the profile shapes by constraining the lattice parameters (pattern matching).

The intrinsic broadening of the reflection lines of $PbK_2LiNb_5O_{15}$ can be obtained by fitting the full widths at half maximum of the gaussian and lorentzian components H_G and H_L of the profile functions. The instrument broadening has been corrected.

The gaussian component is given by $H_G^2 = U\tan^2\theta + \frac{I_G}{\cos^2\theta}$ and the lorentzian by $H_L = X\tan\theta + \frac{Y}{\cos\theta}$. Four parameters are introduced and have been refined independently. The parameters U and X express the effects related to the microstress and the parameters I_G, Y the effects related to the crystallites size. Table 1 summarizes the results of the microstructural analyses.

The value of parameter U for the (00ℓ) reflection is higher comparatively. So, the effect of stress appears to be dominant and leading to a gaussian broadening of Bragg reflection. The Williamson-Hall diagram which represents the reciprocal integral width $\beta^* = \beta\frac{\cos\theta}{\lambda}$ as a function of $d^* = \frac{\sin\theta}{\lambda}$ is

Table 1 Profile parameters associated with the two contributions to the line broadening.

profile parameters	value for the two types of reflections	R_p (%)	R_{wp} (%)	χ^2
without object (whole diagram)	–	7.66	9.75	2.30
U	$U_{(00\ell)} = 0.0046(7)$ $U_{(hk\ell)} = 0.0018(2)$	6.84	8.76	1.86
X	$X_{(00\ell)} = 0.0162(7)$ $X_{(hk\ell)} = 0.0062(7)$	7.29	9.22	2.06
I_G	$I_{G(00\ell)} = 0.0002(1)$ $I_{G(hk\ell)} = 0.0001(1)$	7.52	9.52	2.19
Y	$Y_{(00\ell)} = 0.0023(7)$ $Y_{(hk\ell)} = 0.0005(4)$	7.54	9.51	2.19

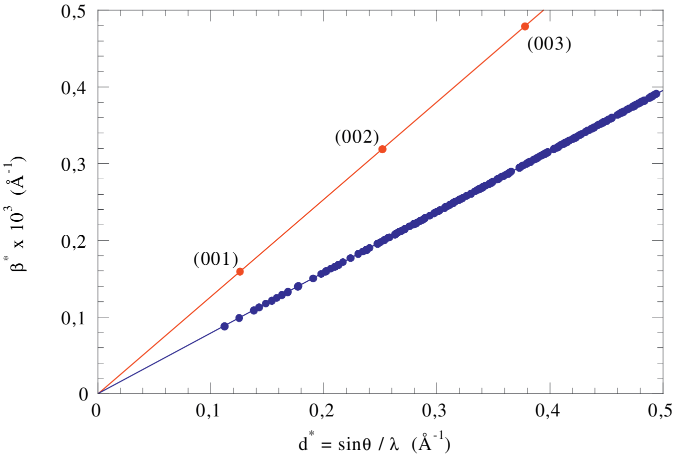

Fig. 2 (online colour at: www.pss-b.com) Williamson-Hall diagram $\beta^* = f(d^*)$ for two kinds of reflections: (00ℓ) and the others.

shown in the Fig. 2 for two kinds of reflections: (00ℓ) and the others. The diagram $\beta^* = f(d^*)$ exhibits two straight lines with two different slopes, the slope for the (00ℓ) lines being the larger. This indicates that the larger the stress state, the larger the micro strains δu_z in the (001) direction, shown also by larger slope.

The crystallites of $PbK_2LiNb_5O_{15}$ are platelet-shaped with the *c*-axis perpendicular to the largest faces. The broadening of the Bragg reflections expresses the presence of microstrains in the sample that are more pronounced along *c*-axis, most probably related to mosaïcity of the grains.

3.1.2 Structural refinement by profile adjustment

The crystallographic structure of the paraelectric phase was refined using the Rietveld method available in the program *Fullprof* [13]. The structural description of the paraelectric phase of $Pb_2KNb_5O_{15}$ given by Sciau et al. in the group *P4/mbm* was used as a starting model [8]. The cell parameters were: $a_t = b_t = 12.6495(4)$ Å and $c_t = 3.9719(4)$ Å. Two sets of reflections were introduced and simultaneously fitted in order to take into account the broadening of the (00ℓ) reflections previously mentioned. At the beginning of the refinement, the Li atoms were not introduced in the model and the Pb^{2+} and K^+ cations were supposed to be on the same crystallographic sites. The refinement of the lattice constants, atomic coordinates, isotropic atomic displacement parameters and chemical occupancies led to a rapid convergence. Nevertheless, a much better fit was obtained when the atomic positions of the Pb^{2+} and K^+ cations in the pentagonal sites, noted Pb2 and K2, were independently refined; the Pb^{2+} and K^+ cations of the square sites (noted Pb1 and K1) remaining on their high symmetry position. The splitting of the cationic sites led to satisfactory reliability factors: $R_{\mathrm{Bragg}} = 4.7\%$ and $R_F = 4.9\%$. The best fit was achieved by refining the anisotropic atomic displacement parameters for the Pb2 atoms. By introducing one lithium atom per formula unit (so that half of triangular sites is occupied), the final reliability factors are: $R_p = 6.3\%$, $R_{wp} = 8.3\%$, $R_{\mathrm{Bragg}} = 4.3\%$, $R_F = 4.6$ % and $\chi^2 = 1.68$. Figure 3 shows observed and calculated X-rays powder diffraction profiles and their difference curve at 670 K.

We present in Table 2, the main obtained parameters derived from the structural refinement and in Table 3, the atomic positions in the framework of $PbK_2LiNb_5O_{15}$ structure.

The refinement of the structure in the tetragonal space group *P4/mbm* being satisfactory with a remarkable agreement between the result of the fit and the experimental profile, the Fourier maps [14] (Fig. 4) have been drawn using observed structure factors and calculated phases.

The Fourier map in the (**a**, **b**) plane shows at 670 K the electronic densities of Pb, K and O atoms at $z = 1/2$. The Pb1/K1 atoms are placed in the tunnels with square sections whereas the Pb2/K2 atoms occupy the tunnels with pentagonal sections. The splitting of the cations around the Pb2/K2 site is exhibited through the elongated electronic densities.

The refinement of the chemical occupancies of the Pb and K atoms allowed:

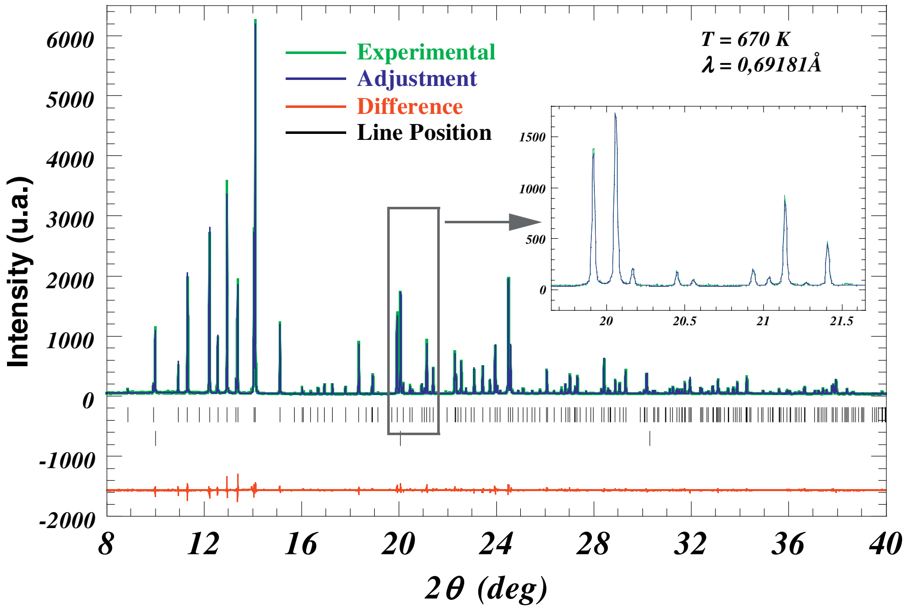

Fig. 3 (online colour at: www.pss-b.com) Observed and calculated X-ray powder diffraction profiles, their position, and the difference curve for $PbK_2LiNb_5O_{15}$ at 670 K (synchrotron radiation data). The inset represents observed and calculated profiles in a limited region.

(i) to precise the distribution of the Pb^{2+} and K^+ cations over the pentagonal and square sites: it is necessary to introduce two disordered positions around K that can be occupied equiprobably by Pb.

(ii) to confirm the overall composition: it appears that 55% of the square sites are occupied by Pb atoms whereas 76% of the pentagonal sites are occupied by K atoms.

From the refined chemical occupancies of Pb and K, the general formula is $Pb_{1.02}K_{1.98}LiNb_5O_{15}$.

3.2 Ferroelectric phase

The structure of the low temperature ferroelectric phase of $PbK_2LiNb_5O_{15}$ was studied by starting with the orthorhombic space group *Pba*2, that was unambiguously deduced from a single crystal diffraction study [11]. In studies performed with single crystals, it is however difficult to overcome the complexity due to absorption and to the complex ferroelastic domain structure to solve the structural problem. The analysis performed with the Jana software allowed nevertheless to conclude that *Pba*2 is the space group.

Table 2 Obtained parameters from the structure refinement of the paraelectric phase.

space group	*P*4/*mbm*
lattice parameters	$a_t = b_t = 12.6490(5)$ Å and $c_t = 3.9711(8)$ Å
chemical occupancy of Pb and K on the square (s) and pentagonal (p) sites	(s_1) 54% of Pb and 46% of K (p_2) 24% of Pb and 76% of K
R_p (%) and R_{wp} (%)	6.3 and 8.3 respectively
R_{Bragg} (%) and R_F (%)	4.3 and 4.6 respectively
χ^2	1.68
number of generated reflections	372
number of refined parameters	60
general formula deduced	$Pb_{1.02}K_{1.98}LiNb_5O_{15}$

Table 3 Atomic positions of $PbK_2LiNb_5O_{15}$ in the paraelectric phase at 670 K; with *P4/mbm* space group.

atoms	x	y	z	B_{iso} (Å^2)	occup.	
Pb1	0	0	0.5	2.53(4)	0.069	square sites (s_1)
K1	0	0	0.5	1.68(5)	0.056	
Pb2	0.1517(8)	0.7045(8)	0.5	6.54(2)	0.059	pentagonal sites (p_2)
K2	0.1624(3)	0.6624(3)	0.5	3.24(9)	0.191	
Nb1	0	0.5	0	1.69(3)	0.125	
Nb2	0.0749(2)	0.2104(4)	0	1.40(9)	0.500	
Li	0.6198(7)	0.1198(7)	0.5	2.00(0)	0.125	1 triangular site on 2 is occupied
O1	0	0.5	0.5	1.76(8)	0.125	
O2	–0.0026(5)	0.3430(5)	0	2.80(1)	0.500	
O3	0.0726(8)	0.2107(5)	0.5	2.43(8)	0.500	
O4	0.2871(6)	0.7871(6)	0	2.04(3)	0.250	
O5	0.1403(9)	0.0674(1)	0	2.02(4)	0.500	

Diffraction diagrams recorded at high (670 K) and at low temperature (290 K) in para and ferroelectric phases respectively, present clear differences (Fig. 5) not only due to lattice parameter changes, but also to the structure change itself.

Figure 6 shows the best result for calculated and observed X-rays powder diffraction profiles and their difference curve at 290 K with *Pba*2 as space group.

The agreement is convincing and the structural results are quite acceptable.

It is noteworthy that again a splitting of Pb^{2+} and K^+ cations positions in the pentagonal sites is necessary to obtain reasonable reliability factors: all other possibilities excluding such a splitting give clearly much worse results, and have to be ruled out. Table 4 gives the result of the structural refinement of the ferroelectric phase. We present in Table 5 the atomic positions for $PbK_2LiNb_5O_{15}$ structure in the *Pba*2 space group.

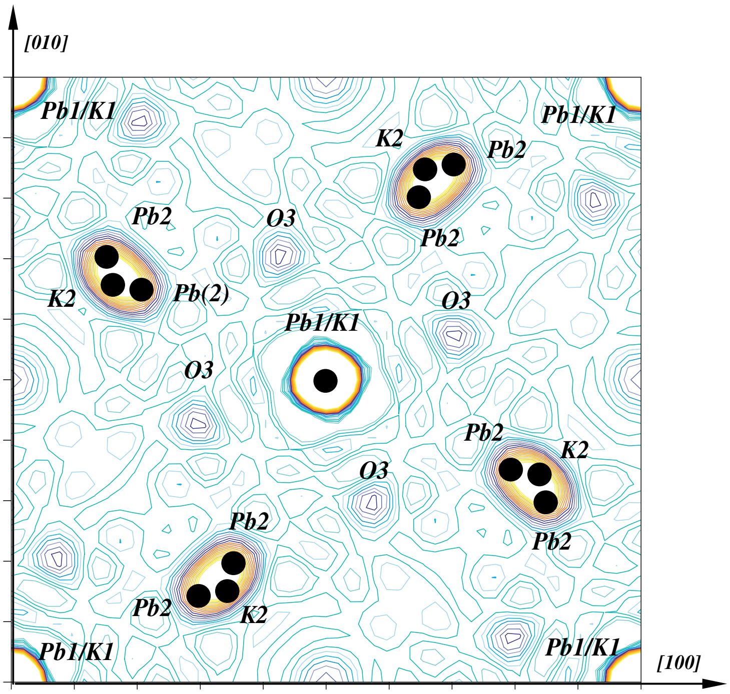

Fig. 4 (online colour at: www.pss-b.com) Fourier map in the (**a**, **b**) plane at $z = 1/2$.

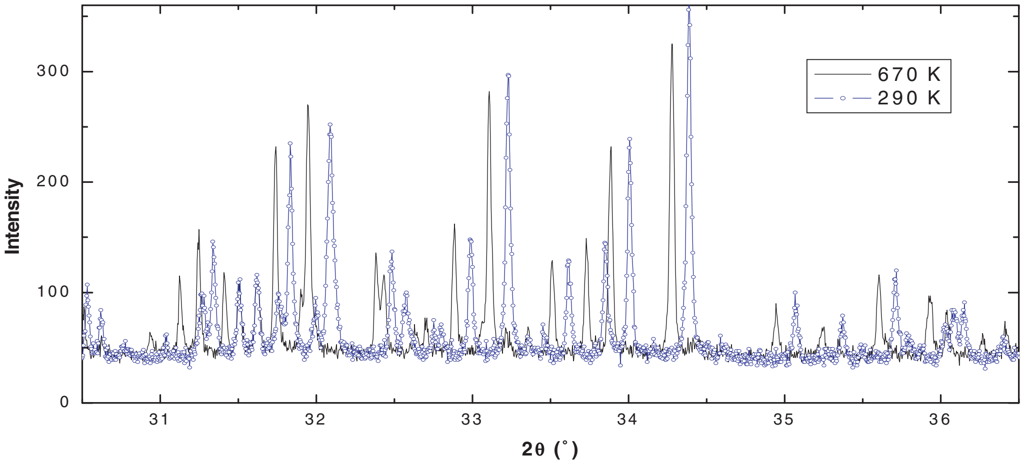

Fig. 5 (online colour at: www.pss-b.com) Comparison of diffraction profiles of high (670 K) and low (290 K) temperature phases in a narrow region. Note that the differences are not only due to a lattice parameter thermal change, but also to the structure change itself (some reflections are splitted, intensities are different, etc.).

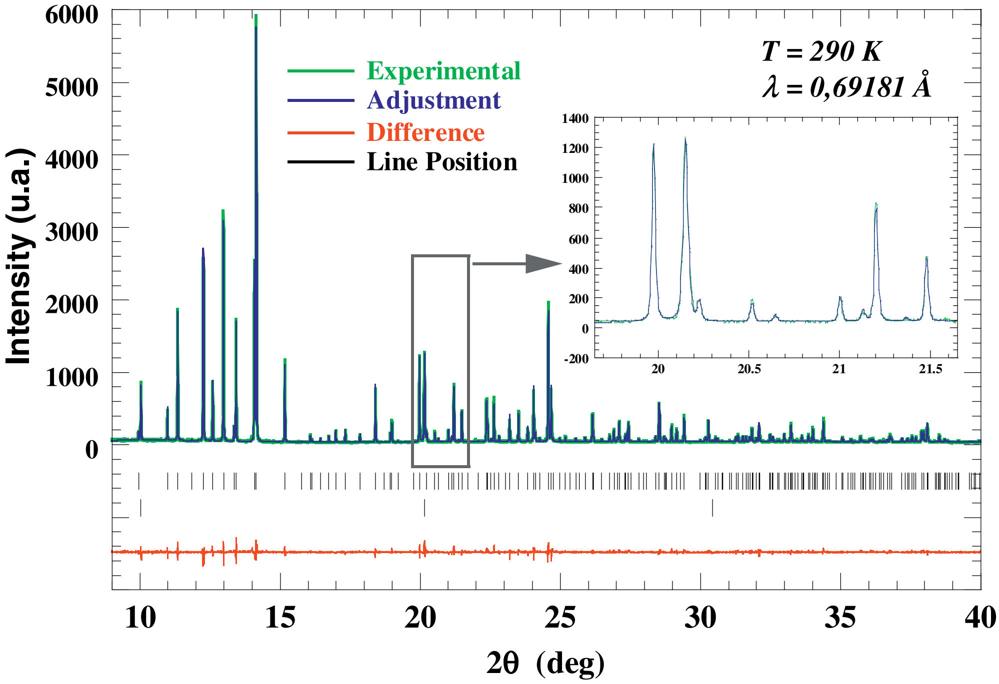

Fig. 6 (online colour at: www.pss-b.com) Observed and calculated X-ray powder diffraction profiles, their position, and their difference curve for $PbK_2LiNb_5O_{15}$ at 290 K (synchrotron radiation data). The inset represents observed and calculated profiles in a narrow region, it is interesting to compare it with the inset of Fig. 3.

Table 4 Structural refinement of the ferroelectric phase with the *Pba*2 orthorhombic space group.

space group	*Pba*2
lattice parameters	a = 12.6122(3) Å b = 12.6128(7) Å c = 3.9541(1) Å
chemical occupancies of Pb and K atoms over the square (s) and pentagonal (p) sites	(s_1) 54% Pb + 46% K (p_2) 26% Pb + 74% K
R_p and R_{wp} (%)	7.6 and 9.8
R_{Bragg} (%) and R_F (%)	5.2 and 7.5
χ^2	2.37
number of generated reflections	372
number of refined parameters	60
general formula	$Pb_{1.05}K_{1.95}LiNb_5O_{15}$

Table 5 Atomic positions obtained in the *Pba*2 space group.

atoms	*x*	*y*	*z*	B_{iso} (Å^2)	occup.	
K1	0	0	0.4293(2)	1.62(3)	0.231	square sites (s_1)
Pb1	0	0	0.5056(8)	1.62(3)	0.269	
K2	0.2056(9)	0.6435(9)	0.4988(8)	5.07(8)	0.743	pentagonal sites
Pb2	0.1576(3)	0.6792(1)	0.5035(8)	5.07(8)	0.257	(p_2)
Nb1	0	0.5	0	1.36(7)	0.500	
Nb21	0.0753(1)	0.2108(5)	–0.0056(9)	1.49(4)	1.000	
Nb22	–0.2108(7)	0.0746(8)	–0.0059(5)	1.30(7)	0.500	triangular site
Li	0.8773(9)	0.6184(6)	0.5	1.00(1)	0.500	1 atom per
O11	0.3490(4)	0.0005(1)	0.0365(3)	2.10(6)	1.000	unit formula
O12	–0.0040(1)	0.3401(5)	0.0429(5)	2.10(6)	1.000	
O21	0.1441(1)	0.0685(9)	0.0205(8)	2.10(6)	1.000	
O22	–0.0664(8)	0.1382(1)	0.0365(1)	2.10(6)	1.000	
O3	0.2137(5)	0.2865(2)	0.0332(5)	2.10(6)	1.000	
O4	0	0	0.5210(5)	2.10(6)	0.500	
O51	0.2780(4)	0.4327(2)	0.5157(5)	2.10(6)	1.000	
O52	–0.4184(7)	0.3030(5)	0.5078(8)	2.10(6)	1.000	

Figure 7 presents the Fourier map [14] drawn in a plane perpendicular to the *c*-axis at $z = 1/2$, calculated from the *Pba*2 space group. It is rather similar to the one obtained in the high temperature paraelectric phase (Fig. 4) but the difference of disorder of Pb and K atoms is clearly seen.

From the structure result, it appears that the tunnels with pentagonal sections are mainly occupied by K atoms (average occupancy of 76%) whereas the square sites are preferentially occupied by Pb atoms (54% for Pb against 46% for K). One can notice that the deduced proportion of the Pb^{2+} and K^+ cations over the pentagonal and square sites is very close to the one determined from the structural refinement of the paraelectric phase, which a posteriori validates the structure results for both phases.

Following the work of Sciau et al. in $Pb_2KNb_5O_{15}$ [8], we tested if it is possible to refine the structure in the alternative *Cm*2*m* space group in which the a and b axes are rotated by 45° around the *c*-polar axis (the cell parameters *a* and *b* are then multiplied by $\sqrt{2}$) with respect to the formers. From a purely crystallographic study, the results of structure refinement are nearly equally satisfying for both space groups.

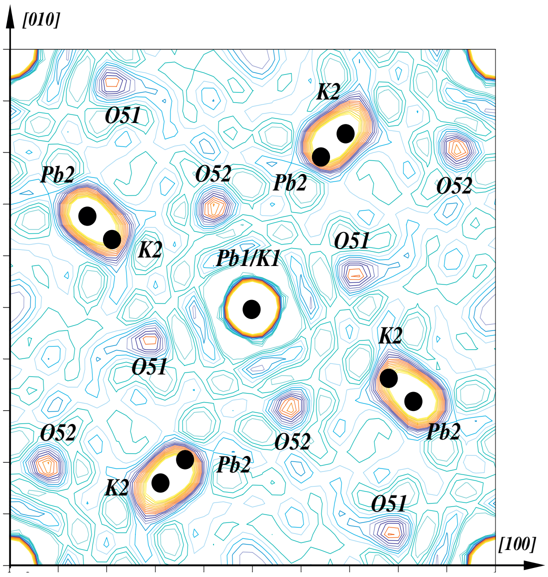

Fig. 7 (online colour at: www.pss-b.com) Fourier map drawn in a plane perpendicular to the c-axis at $z = 1/2$ ($Pba2$ space group). The crystallographic directions are given with respect to the unit cell of the paraelectric phase.

The major difference between both groups is the number of (distorted) pentagonal sites occupied by Pb and K ions in the lattice: 1 in $Pba2$ and 3 in $Cm2m$.

Comparable reliability factors [13] indicate that both structures for the ferroelectric phase of $PbK_2LiNb_5O_{15}$ are in principle acceptable in the frame of the Rietveld method. Nevertheless the number of refined parameters is larger for $Cm2m$ (78) than for $Pba2$ (60) whereas the difference of reliability factors is rather small. The $Cm2m$ group may be definitely excluded here on the basis of ferroelectric properties, and also of HREM image analysis [15]. The difference of atomic positions is tiny between both structures but the difference of physical properties is significant: in $Pba2$, the polarization is directed along the $[001]_O$ (orthorhombic) axis, which coincides with the $(001)_t$ (tetragonal) axis. In $Cm2m$, the polarization is along the $(010)_O$ (orthorhombic) axis which is perpendicular to the $(001)_t$ direction. Ferroelectric properties of both structures (with $Cm2m$ and $Pba2$ space groups) present therefore clearly different features. We know that the crystal grows as platelets [9], the c crystallographic vector being perpendicular to the large faces. In the case of the structure corresponding to $Pba2$, the polarization thus lies in the direction perpendicular to the large crystal faces in agreement with dielectric measurements. In $Cm2m$, the polarization would be parallel to the platelet so that the ferroelectric space group $Cm2m$ is excluded.

4 Conclusion

The detailed structural characterisation of $PbK_2LiNb_5O_{15}$ structure has been performed successfully using the Rietveld method. Atomic positions and the distribution of the different cations within the tunnels in the structure have been determined. Though the structural study performed on powder would reveal an ambiguity for the solution, only one space group can be retained on the basis of the comparison between expected and observed dielectric properties. The ferroelectric structure is with the space group $Pba2$. This is also in agreement with the conclusion driven from a study performed by HREM. The detailed discussion of the properties of the phase change that occurs in $PbK_2LiNb_5O_{15}$ between para- and ferroelectric phases will be given in another paper. From the present study, it is noteworthy that both polar displacements and the ferroelastic strains are tiny at room temperature.

Acknowledgements This work was supported by NATO collaborative linkage grant PST.CLG.980055.

References

[1] A. Magnéli, Ark. Kemi **1**, 213 (1949).

[2] J. Ravez, A. Perron-Simon, and P. Hagenmuller, Ann. Chim. **t.I**, 251 (1976).

[3] M. E. Lines and A. M. Glass, Principles and Applications of Ferroelectrics and Related Materials (Clarendon Press, Oxford, 1977).

[4] J. Ravez and B. Elouadi, Mater. Res. Bull. **10**, 1249 (1975).

[5] A. Perron-Simon, G. Demazeau, J. Ravez, and P. Hagenmuller, C. R. Acad. Sci. (Paris) **281**, 351 (1975).

[6] Ph. Labbé, M. Frey, B. Raveau, and J. C. Monier, Acta Cryst. B **33**, 2201 (1977).

[7] Z. G. Lu, J.-P. Bonnet, J. Ravez, and P. Hagenmuller, Eur. J. Solid State Inorg. Chem. **30**, 817 (1993).

[8] Ph. Sciau, G. Calvarin, and J. Ravez, Acta Cryst. B **55**, 459 (1999).

[9] Y. Gagou, D. Mezzane, N. Aliouane, T. Badèche, M. Elaatmani, M-H. Pischedda, and P. Saint-Grégoire, Ferroelectrics **254**, 197 (2001).

[10] D. Mezzane, Y. Gagou, N. Aliouane, A. Flory, T. Badèche, A. Zegzoutti, and P. Saint-Grégoire, Izv. Akad. Nauk, Ser. Fiz. **65**, 1134 (2001).

[11] Y. Gagou, D. Mezzane, N. Aliouane, J. Fabry, T. Badèche, E. Zegzouti, M. Lopez, and P. Saint-Grégoire, Ferroelectrics **251**, 131 (2001).

[12] H. M. Rietveld, J. Appl. Cryst. **2**, 65 (1969).

[13] J. Rodriguez-Carvajal, "Fullprof", Satellite Meeting on Powder Diffraction of the XVth Congress International Union of Crystallography, 127 (1990).

[14] J. Gonzalez-Platas and J. Rodriguez-Carvajal, Graphic Fourier Program (2000).
http://www-llb.cea.fr/fullweb/others/newfour.htm

[15] T. Badèche, Y. Gagou, C. Roucau, M. A. Frémy, D. Mezzane, and P. Saint-Grégoire, Ferroelectrics **290**, 83 (2003).